Available online at www.sciencedirect.com

ScienceDirect

Procedia Manufacturing 42 (2020) 211–218

Procedia MANUFACTURING

www.elsevier.com/locate/procedia

International Conference on Industry 4.0 and Smart Manufacturing (ISM 2019)

An embedded machine vision system for an in-line quality check of assembly processes

Fabio Frustaci[(a)(*)], Stefania Perri[(b)], Giuseppe Cocorullo[(a)], Pasquale Corsonello[(a)]

[a]*DIMES Department, University of Calabria, Via P. Bucci, Arcavacata di Rende (CS)87036, Italy*
[b]*DIMEG Department, University of Calabria, Via P. Bucci, Arcavacata di Rende (CS)87036, Italy*

* Corresponding author. Tel.: +39-0984-494647; *E-mail address:* f.frustaci@dimes.unical.it

Abstract

In the context of the Industry 4.0 and Smart Manufacturing paradigm, this paper proposes a machine vision system for a flexible, precise and low-cost in-line geometric inspection of assembly processes. As a case study, the system has been targeted to the catalytic converter assembly process, in order to be easily integrated in the consolidated manufacturing flow. The system is based on developed algorithms to be applied on the image of the interfaces with the complete exhaust system the catalytic converter will be assembled into. An image segmentation procedure is described to robustly identify the region of interest (ROI) in the image. Afterwards, a geometrical model is proposed to detect any possible geometrical defects due to planar and/or rotational shifts of the interfaces around their expected positions. For the sake of validation, the proposed system has been implemented on a Raspberry Pi 3 Single Board Computer (SBC). It showed a sub-millimeter precision for planar movements and a maximum error in detecting the rotation angle lower than 1 degree, respectively. The modularity of the proposed approach makes it suitable to be realized also on different computational platforms, such as the modern heterogeneous System-on-Chips (SoC) hosting a general purpose microprocessor and a Field Programmable Gate Array (FPGA) on the same chip. Indeed, the most time-consuming computational steps can be efficiently realized on the FPGA, exploiting the parallel computing capability offered by a hardware implementation, thus accelerating the overall computation.

Keywords: Machine vision; in-line inspection; non-contact measurement; automation; catalytic converter assembly

1. Introduction

Each manufacturing process is continuously required to boost its efficiency to remain competitive in its market sector. In order to do that and according to the Industry 4.0 and Smart Manufacturing paradigm, today's industrial productive systems should activate a series of processes bringing their traditional industrial automation towards a form of digital integration of all its components. More importantly, there is the need for new low-cost digital automation techniques that can be efficiently integrated in the existing productive process without requiring its complex re-engineering.

Inspection, measurement and fault detection are commonly used control procedures whose importance is crucial in almost every industrial assembly process [1]. Typically, the geometric inspection of the assembled units is not automated but it is still undertaken at the end of the manufacturing process by the operator who manually uses specialized instruments, such as steel rules, micrometers and calibers which all require a direct physical contact. Such an approach has some evident drawbacks: it is time consuming, it can be applied just on one single sample over a set within the production lot and it may be subject to human errors. Moreover, the data of the process quality can not be efficiently collected, thus preventing a predictive maintenance based on big data analysis. For all these

10.1016/j.promfg.2020.02.072

reasons, the development of a digital system aiming to automatically inspect the geometric compliance of the assembled units with non-contact methods can drastically boost the process productivity. The use of 3D optical digitizing techniques as contactless measurement methodologies has been investigated in several industrial processes [2]-[3]. The drawback of such a technique is the need for rotating tables in order to get the 3D rendering of the object, which can be very hard to be integrated into the consolidated flow of the manufacturing process. A similar existing commercial solution is based on 3D laser triangulation to construct a 3D point cloud of the catalytic converter [4]. However, its main goal is to replace expensive and inflexible gauges but it cannot be easily integrated in an existing process due to its high measuring time (order of minutes) and the need for a motion system. Moreover, measurements on the virtual 3D model of the assembled unit are not automated but an operator still has to manually choose two points on the model surface to measure their relative distance. Therefore, such a methodology is not suitable for an in-process inspection.

Machine vision has been widely recognized as an effective contactless technology for automated geometric inspection [5]-[17]. Essentially, machine vision is based on the acquisition of an image from a camera and on its elaboration through image processing algorithms for some specific tasks, such as image analysis and feature extraction. In [8], the Fast Localization with Advanced Search Hierarchy (FLASH) algorithm is proposed which is based on image comparison to detect geometrical deviations from a reference pattern. The paper [7] describes a framework to measure the object movement from a pixel level analysis of the captured images. The work in [9] proposes the use of a stereo pair camera to obtain the 3D coordinates of a reference point from two 2D images. Although such automation strategies achieve a very good spatial resolution (< 1mm), they have some geometrical limitations: they work supposing that the observed object can move only on a plane and/or they take into account possible rotation of the object around only an axis orthogonal to the reference plane.

In this paper, we investigate the possibility to use a machine vision system for a flexible, precise and low-cost in-process geometric inspection of assembled units that can be easily integrated in the consolidated manufacturing process flow. The production of close-coupled catalytic converters is taken as a case study since it is a significant example of industrial application where the geometric inspection is of fundamental importance. As part of the exhaust system, catalytic converters belongs to the standard equipment of cars with internal combustion engines. They are manufactured by joining individual components together and the quality of the welding process has a direct impact on the converter flanges capability to fit the complete exhaust system to be assembled later.

We developed a geometrical model in order to detect both planar and rotational movements of the flanges. In order to demonstrate its effectiveness, the model has been included in software routines based on an open source computer vision library [18], showing a sub-millimeter precision for planar movements and a maximum error in detecting the rotation angle lower than 1 degree. The machine vision system has been implemented on an embedded system based on the Raspberry Pi 3 Single Board Computer (SBC) equipped with the 1.4 GHz 64- bit Cortex-A53 SoC with the aim to send the computational results online to a server, where they can be further elaborated offline. It is worth noting that the proposed system is general and that it can be implemented on different computing platforms, according to the required computational needs. As an example, a hardware-software co-design approach can be used on platforms hosting a heterogeneous System on Chip (SoC), as the Xilinx® Pynq [19], where a general purpose microprocessor and a Field Programmable Gate Array (FPGA) are integrated into the same chip. On such a platform, some time-consuming functions can be described in a hardware description language (HDL) and they can be realized in hardware accelerators into the FPGA, thus considerably speeding-up the overall computation. Indeed, several operations on images, such as filtering, can efficiently exploit the typical parallel computing capability offered by a hardware implementation. Conversely, non-critical functions can be implemented in software running on the general purpose processor, thus exploiting the typical flexibility of the high-level programming languages that can easily describe complex computational procedures, use efficient data structures and import third-part libraries.

The paper is organized as follows: in Section 2, the manufacturing process of the catalytic converters is briefly described; Section 3 discusses the proposed methodology for the flange detection using image segmentation; In Section 4, the proposed geometrical models for the detection of planar and rotational movements are described and the obtained experimental data are discussed; finally, conclusions and future work are described in Section 5.

2. The catalytic converter assembly process

The assembly of a catalytic converter is essentially based on two processes: sensor bosses welding and clamshell welding assembly. Most of the sensor bosses Metal-Active-Gas (MAG) welding processes develop in parallel on the two different clamshells. The latter are then assembled together with semiautomatic Metal-Inert-Gas (MIG)/ Metal-Active-Gas (MAG) welding. Finally, the Selective Catalytic Reduction on Filter (SCRoF) chamber is welded with the clamshells and the input and output collectors, and the final converter is then placed in a quality cell for a leakage test that takes about one

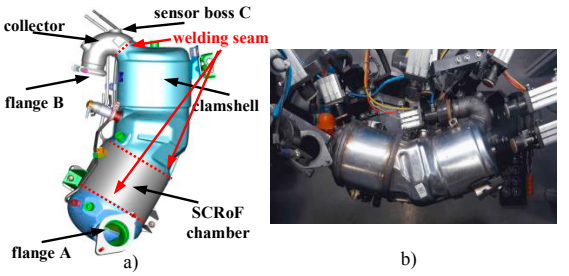

Fig. 1: a) the assembled catalytic converter and b) its placement into the quality cell (courtesy of Magneti Marelli CK Holdings)

minute and a half (Fig. 1). Afterwards, the converter is sent for the assembly of the heat shield and brackets and then it is ready for packaging. The described welding processes affects the converter quality. The geometrical inspection of the converter shown in Fig. 1 is currently performed only on a single sample over a predefined set within the production lot. When the inspection occurs, the converter is placed into a specialized cell equipped with special calibers, which are used by a human operator, and the production is stalled, with a consequent waste of time. More importantly, this offline check can not detect any possible defects on the previously assembled converters, with the risk of wasting a considerable number of units. Finally, the statistics of the process is incomplete preventing a meaningful offline analysis aiming to efficiently monitor the quality of the entire production flow for the purpose of a predictive maintenance. For all these reasons, the analyzed machine vision system is intended to be integrated into the existing quality cell entailing an in-line check of the geometric compliance of each assembled converter. The real-time feature of the proposed system avoids slowing down the manufacturing flow and it overcomes the drawbacks of the manual inspection described above.

Essentially, the most important geometrical check is to detect the correct position of the flanges A and B depicted in Fig. 1a, which are the interfaces with the complete exhaust system the converter will be assembled into. As it is visible in Fig. 1b, the flange B is not visually accessible when the converter is placed in the quality cell. Consequently, we propose to monitor the correct position of the sensor boss C since it is not subject to welding but it is monolithically realized on the collector thus resulting rigidly coupled with the flange B. In the following, the developed procedures to detect the flange and/or the sensor boss in an image and their possible movement with respect to the expected position will be described.

3. The image segmentation procedure

Image segmentation is the first elaboration step on the acquired image. It consists in detecting the region of interest (ROI) and isolating it from the rest of the image. Without loss of generality, in the following we will describe the proposed segmentation method to detect the sensor boss C, with the obvious assumption that the same procedure can be applied by a replica of the system also to the flange A of Fig. 1a.

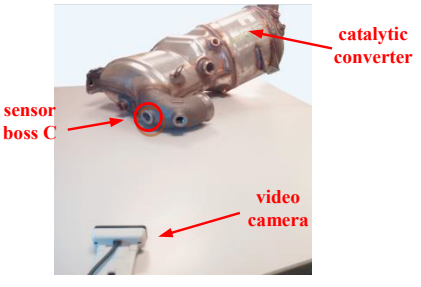

Fig. 2: Experimental setup (catalytic converter courtesy of Magneti Marelli CK Holdings).

The basic components of the embedded machine vision system are: a Single Board Computer (SBC) and a video camera. A C++ software routine runs on the SCB's processor and performs the image acquisition through the video camera making use of useful machine vision functions furnished by the open source OpenCV 3.2.0 library. Nevertheless, due to its modularity, the proposed approach can be also efficiently implemented in heterogeneous SoC, once the critical functions to be implemented in hardware have been identified. Figure 2 shows the experimental setup for the image acquisition and segmentation consisting in the used video camera (Microsoft VX-500 USB LifeCam) and the catalytic converter. In the following, the main computational steps of the proposed procedure are listed and described:

1) **Color image acquisition** from the video camera. The chosen image resolution is 640x480.

2) **Image conversion** from the RGB color space into the Grayscale. After this step, each pixel of the image is coded with an integer number belonging in the range [0 – 255] (0 for full black, 255 for full white). In order to reduce the computation complexity, the likely region of interest (ROI) is selected from the grayscale image and isolated. For our experimental setup, a ROI dimension of 140x120 pixels has been found to be appropriate to contain the shape of the sensor boss C. It is worth noting that the ROI selection (specifically, its dimension and position within the original image) can be easily done since the camera-sensor boss relative position is a chosen specification of the experimental setup. The output of this computational step is depicted in Figure 3a.

3) **ROI filtering** to remove noise and to detect edges within the ROI. A median filter removes the noise from the image by substituting the value of the generic pixel *P* with the

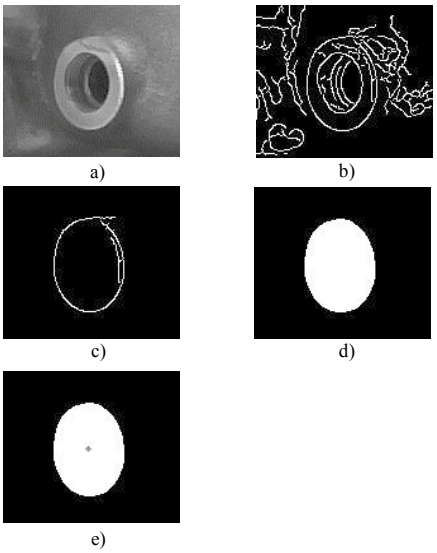

Fig. 3: Outputs of the proposed image segmentation procedure on the sensor boss: a) grayscale conversion, b) ROI filtering; c) contour selection; d) morphological filtering; e) center detection.

median value among the pixels belonging to a squared window centered in *P*. For our case study, a window length of 5 pixels has been found appropriate. In order to detect the edges within the ROI, a Canny filter [20] has been employed. The lower and upper thresholds of the Canny edge detection filtering have been empirically set to 10 and 50, respectively. The output of this computational step is depicted in Figure 3b. It is worth noting that the resulting image is segmented since all the pixels belonging to the edges assume the same value 255 (i.e. white), whereas the remaining ones get the same value 0 (i.e. black).

4) **Contour selection** of the object of interest. As it is visible in Figure 3b, the Canny algorithm detects several edges besides the ones belonging to the object of interest (the sensor boss C). This is due to the presence of irregularities on the metallic collector and/or small shadows caused by the illumination. With a careful choice of the ROI dimension, it can be reasonably inferred that the contour to be actually detected is the one with the largest length among all the contours of Figure 3b. Towards this aim, all the contours in the segmented image are collected into a data structure and only the one with the largest length is selected. The output of this computational step is depicted in Figure 3c.

5) **Morphological filtering** of the selected contour. This computational step aims to remove some undesired textures that are still present in the image [10]. A clear example is visible in Figure 3c, where the selected contour is a line that a) does not delimit an enclosed area and that b) contains a fringe due to surface irregularities and/or illumination effects. To solve the problem a), a morphological dilatation with a kernel size 3x3 has been applied. Dilatation thickens the selected contour so that it can delimit an enclose area. Afterwards, the enclose area is filled with the same color (i.e. all the pixels inside the area are set to the same value – 0 for white –). The inverse of dilatation, i.e. erosion, has been then applied to the enclose area with the same kernel size 3x3. To solve problem b), we have applied two consecutive erosion and dilation operations with a larger kernel size (we found that the kernel size 21x21 is appropriate): the erosion operation eliminates the fringe whereas the dilatation operation restores the original object size. Figure 3d depicts the final output.

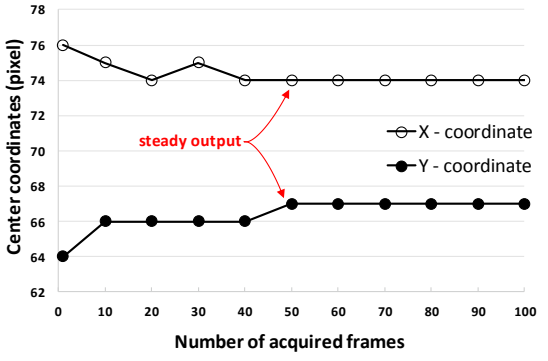

Fig. 4: The detected coordinates of the sensor boss center after the proposed averaging operation as a function of the number of acquired frames.

6) **Center detection** of the enclose area. This is the final computation step aiming to identify the coordinates of the center of the enclose area in the 2D camera plane. Through a connected components analysis of the image, the (single) connected component has been identified and its center has been detected (Figure 3e).

In order to make the described procedure more robust, we propose to iterate it over a set of consecutive acquired frames and to evaluate the coordinates of the center by averaging the obtained results [11]. Indeed, due to imperceptible micro variations of the illumination condition over time, the output of the ROI filtering step may result different even for the same object if it is detected in different times. Moreover, in our experiment we noticed that, for the same reason, the actual contour of the sensor boss was not detected at all for some of the acquired frames. As a result, the value of the coordinates of the center was clearly unreasonable. For such a reason, we neglected from the averaging operation those values that were outside a reasonable neighborhood of the expected position of the center. Figure 4 depicts the detected center coordinates as a function of the total number of acquired frames. Our experiments reveal that a number of frames equal to 50 is enough to obtain a steady value of the center coordinates. However, it is worth noting that, using less frames, the maximum error was found to be just of 3 pixels, hence the number of frames to be acquired is also a function of the desired precision.

The obtained center can be used as reference point to detect possible movements of the sensor boss around its expected position, as it will be shown in the following Sections.

4. The proposed machine vision-based geometric inspection

Once the object of interest - i.e. the sensor boss in our case study - has been identified through the segmentation procedure, the next step is to elaborate the segmented image in order to automatically detect a possible incongruity between the actual and the expected object position. As described in Section 2, this may occur when the quality of the welding seams is below an acceptable threshold. Without losing of generality, in this study we suppose that a displacement of the sensor boss can be attributed to a planar and/or rotation movement. In the following, we investigate the possibility to use a machine vision system to detect such movements.

4.1. Planar movements detection

Reasonably, when the catalytic converter enters the quality cell, the sensor boss planarity and size are assumed to be compliant with the standard values since the check of the collector is independently carried out before the assembly

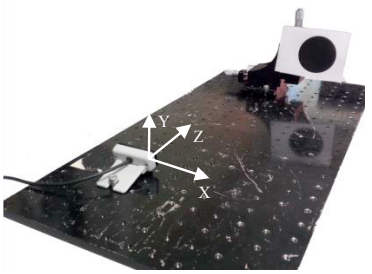

Fig. 5: The experimental environment.

process. Hence, the center of the sensor boss can be used as reference point to detect a rigid planar movement. In order to investigate the feasibility of a machine vision system towards this aim, an experimental environment as the one showed in Figure 5 has been set up. The camera and the target object have been mounted on an optical bench. The camera position is fixed and it is assumed to be a known specification of the system, taken as the origin of the 3D Cartesian space. The target object has the same shape and dimension of the sensor boss and it is mounted on a mechanical carriage that allows controllable and measurable micro movements along the XY plane (with a resolution of tenths of millimeter).

4.1.1. First scenario: the camera and the target object planes are parallel

We started our investigation by studying the simplest case in which the camera and the target object are lying on parallel planes, as depicted in Figure 5. Let's define: (X_p, Y_p) the pixel coordinates of the center in the image plane; (X_W, Y_W) the center coordinates in the real world; Z_0 the camera-object distance in the real world; F the focal length (in pixels) of the camera. According to the pinhole camera model [21], the mapping from the coordinates of a 3D point to the 2D image coordinates of the point's projection onto the image plane is given by Equation 1:

$$\begin{pmatrix} X_p \\ Y_p \end{pmatrix} = \frac{F}{Z_0} \cdot \begin{pmatrix} X_W \\ Y_W \end{pmatrix} \quad (1)$$

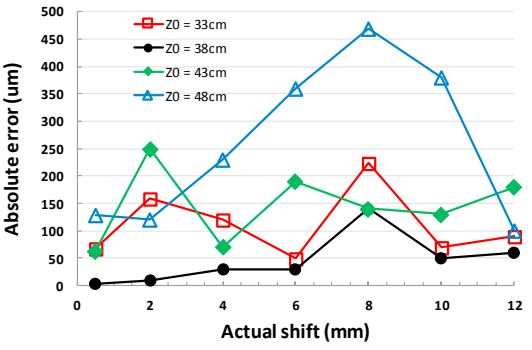

Fig. 6: Measured absolute error when the camera and the object planes are parallel (Equation 2).

From Equation 1, it can be easily inferred that, when the point moves from position A to position B, the movement amount in the real world can be obtained as described by Equation 2:

$$\begin{pmatrix} \Delta X_W \\ \Delta Y_W \end{pmatrix} = \begin{pmatrix} |X_{W,B} - X_{W,A}| \\ |Y_{W,B} - Y_{W,A}| \end{pmatrix} = \frac{Z_0}{F} \cdot \begin{pmatrix} |X_{p,B} - X_{p,A}| \\ |Y_{p,B} - Y_{p,A}| \end{pmatrix} = \frac{Z_0}{F} \begin{pmatrix} \Delta X_p \\ \Delta Y_p \end{pmatrix} \quad (2)$$

Equation 2 has been included in the developed software routine and tested. Figure 6 collects the measurement errors committed by the described procedure, obtained experimentally for different values of Z_0 and object shift in the XY plane. The amount of the object shift has been calculated by measuring the shift of the object center with respect a known position. It is worth noting that the maximum absolute error is always lower than 500um.

4.1.2. Second scenario: the camera and the target object planes are not parallel

Our investigation on the feasibility of the machine vision system continued by removing the parallelism ideality between the camera and the object planes. Indeed, as it can be easily inferred from the position of the catalytic converter in the quality cell of Figure 1b, this may represent a more realistic scenario. The latter has been modelled as depicted in Figure 7. Let's define: α the angle between the camera and the object planes; Z_0 the distance between the object center and camera plane; b the distance between the object center and the point A (aligned with the camera focal point). Let's suppose that the object shifts from the point B to the point D along the direction r by a distance equal to c. After detecting the object center coordinates in the image plane and applying Equation 2, the value a is measured. The latter is not the actual object shift but, according to the pinhole camera model, it is the distance between the points B and C. Under the realistic assumption that Z_0 is much larger than the camera focal length, we can derive the geometrical model described by Equation 3 in order to obtain the actual shift c:

$$\delta = arctg \frac{a + b}{Z_0}$$

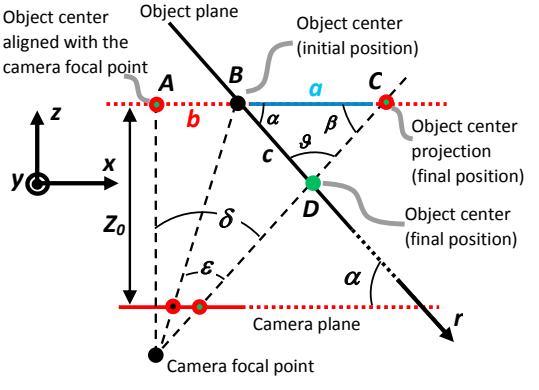

Fig. 7: Geometrical model for the case when the camera and the object planes are not parallel.

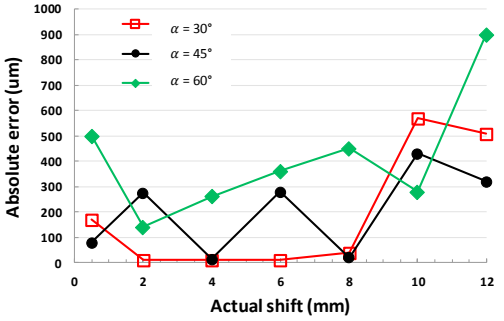

Fig. 8: Measured absolute error when the camera and the object planes are not parallel (Equation 3).

$$\beta = \frac{\pi}{2} - \delta = \frac{\pi}{2} - arctg\,\frac{a+b}{Z_0}$$

$$\vartheta = \frac{\pi}{2} + \delta - \alpha = \frac{\pi}{2} + arctg\,\frac{a+b}{Z_0} - \alpha$$

$$c = a \cdot \frac{sin\beta}{sin\vartheta} = a \cdot \frac{sin\left(arctg\frac{a+b}{Z_0}\right)}{cos\left(arctg\frac{a+b}{Z_0} - \alpha\right)} \qquad (3)$$

Figure 8 depicts the absolute measurement error of the proposed model for different values of α (in the performed experiment, we set b = 5 cm and Z_0 = 48 cm). Also for this scenario, the proposed model achieves a high precision with a maximum error below the millimeter. It is worth noting that the measured absolute error tends to increase with the increasing of the actual shift of the object. Nevertheless, it may confidently be stated that the tolerable sensor boss shifts are below 1 cm, thus the error introduced by the proposed machine vision system is assumed to be not higher than small fractions of millimeter.

4.2. Rotational movements detection

Apart from planar shifts, the sensor boss can also undergo rotational movements due to a low quality of the welding seam. In such a case, the detection of just the center is not enough to evaluate the geometric compliance of the object. As an example, if the object rotates across an axis passing through the center, the latter does not change its position in the real world. As a consequence, the catalytic converter may wrongly pass the quality check. For such a reason, we enriched our machine vision system with the geometrical model described in Figure 9, that is able to detect rotations.

Let's define: ϕ the rotation angle to be detected; Z_0 the distance between the camera and the object planes for ϕ=0; B (D) the point representing the left border of the object for ϕ=0 (ϕ>0); a the distance between the points B and A (aligned with the camera focal point). Let's suppose that, due to a rotation of an angle ϕ, the left border of the object D is projected onto the image plane in the same position of the projection of the point C. Due to rotation, the sensor boss on the image plane assumes an elliptic shape whose eccentricity depends on the rotation

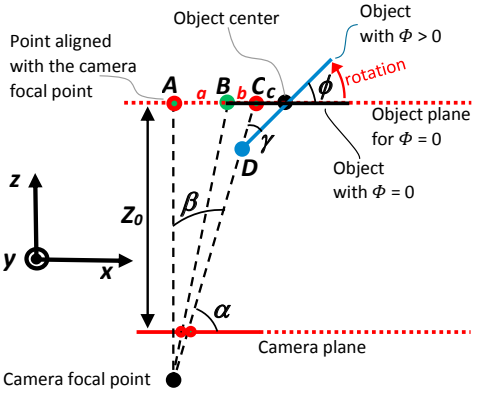

Fig. 9. Geometrical model to detect rotations.

angle. Hence, the length of the segment c can be obtained as the length of one semi axis of such an ellipse. Once the sensor boss has been detected in the image, through the segmentation step described in Section 3, its elliptical shape is matched to a synthetic ellipse. As an example, when implemented in software, such a step can be easily realized with the OpenCV function *fitEllipse*. The latter looks for an elliptical shape in the image, matches it with an ideal ellipse and returns some useful information such as the length in pixels of the concerned semi axis (the segment c). Afterwards, the length in pixels is converted into its actual length in the real world by applying Equation 2. The actual length b in the real world is then easily calculated since the actual length of the sensor boss semi axis is a known system parameter. As a result, the value of the rotation angle ϕ can be found by the following Equation (4):

$$\beta = arctg\,\frac{|b+a|}{Z_0}$$

$$\alpha = \frac{\pi}{2} - \beta$$

$$\frac{c}{sin\gamma} = \frac{b+c}{\sin(\pi-\alpha)}$$

$$\gamma = arcsin\,\frac{c \cdot \sin(\pi-\alpha)}{b+c}$$

$$\phi = \pi - \gamma - (\pi - \alpha) = \alpha - \gamma \qquad (4)$$

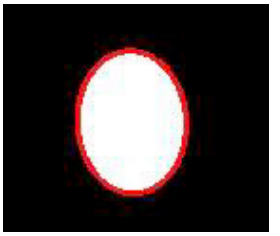

Fig. 10: Elliptical matching (in red) of the sensor boss surface (in white) with the OpenCV function *fitEllipse*.

Figure 10 shows the ellipse (in red) found by the *fitEllipse* function matching the border of the sensor boss (in white). It can be noted how the matching is almost perfect, so the measurement of the segment c can be assumed to be very reliable. Figure 11 depicts the measured absolute error of the proposed model (4) for different values of the actual rotation angle ϕ. The proposed model is able to measure the angle ϕ with a high accuracy, showing a maximum error of just 0.9 degrees.

5. Conclusions and future works

The geometric quality check is an important step in the manufacturing process of catalytic converts. It consists in checking the correct position of the flanges/sensor bosses which are the interfaces with the complete exhaust system. The current procedures require specialized operators and the use of measurement methodologies that are based on a direct physical contact. This prevents the possibility of an in-line quality check on every manufactured converter and the collection of the process statistics for the purpose of a predictive maintenance. In this paper, we investigated the possibility to exploit a machine vision-based system that can be easily integrated into the existing productive flow in order to perform a real time quality check of the catalytic converter. We developed a robust algorithm to correctly detect the border of the flange/sensor boss in an image acquired from a video camera. Afterwards, we modeled the geometry of the case study and we derived some mathematical formula to detect potential geometric defects in the flange/sensor boss due to unwanted planar and rotational movements. The presented system has been prototyped using the Raspberry Pi 3 SBC. Experimental results showed that the proposed methodology is able to detect planar and rotational movements with a maximum error of just 900um and 0.9 degrees, respectively. It is worth noting that the proposed approach is general and that it can be implemented on different platforms. As an example, the modularity of the proposed procedure makes it easy to profile the computational time of each step. Consequently, the time-critical computational steps can be realized and accelerated in hardware into the FPGA resources of modern heterogeneous SoCs.

The high obtained precision reveals the reliability of machine vision as a low-cost and real time quality check methodology of the catalytic converters assembly process. Going through the path indicated by the proposed feasibility study, we are planning to enrich our system with ad-hoc stereoscopic techniques and/or time-of-flight sensors for the purpose of an automatic detection of the camera-object distance. The main goal of our work is to provide the embedded system with the appropriate intelligence to detect any kind of possible object movements in the 3D space.

Acknowledgments

This work was supported by the Italian Ministry of Education (MIUR), PNR 2015-2020 Program under the Grant ARS01_01061

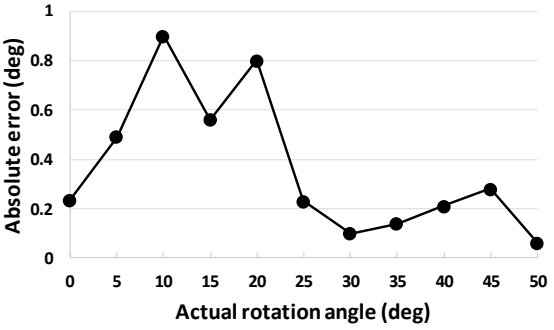

Fig. 11: Measured absolute error of the proposed model to detect rotation (Equation 4).

References

[1] Herakovic N. Robot Vision in Industrial Assembly and Quality Control Processes. Robot Vision. InTech, 2010, pp. 501-534.

[2] Petrišič J, Suhadolnik A, Kosel F. Object Length and Area Calculations on the Digital Images. Proc. of the 12th Inter. Research/Expert Conference "Trends in the Development of Machinery and Associated Technology" TMT 2008, August 26-30, Istanbul (Turkey), pp. 713-716.

[3] Palousek D, Omasta M, Koutny D, Bednar J, Koutecky T, Dokoupil F. Effect of matte coating on 3D optical measurement accuracy. Optical Materials, 2014, 40, pp. 1-9.

[4] OptoInspect 3D Inline, Demo version available from: http://www.optoinspect3d.de/documentation/html/index.html [accessed 3 September 2019].

[5] Dworkin SB, Nye TJ. Image Processing for Machine Vision Measurement of Hot Formed Parts. Journal of Materials Processing Technology, 2006, 174 (1–3), pp. 1-6.

[6] Chen M-C, Tsai D-M., Tseng H-Y. A Stochastic Optimization Approach for Roundness Measurements. Pattern Recognition Letters, 1999, 20, pp. 707-719.

[7] Mahapatra PK, Thareja R, Kaur M, Kumar A. A Machine Vision System for Tool Positioning and Its Verification. Measurement and Control, 2015, 48 (8), pp. 249-260.

[8] Lai S-H, Fang M. A Hybrid Image Alignment System for Fast and Precise Pattern Localization. Real-Time Imaging, 2002, 8, pp. 23-33.

[9] Ngo N-V, Hsu Q-C, Hsiao W-L, Yang C-J. Development of a simple three-dimensional machine-vision measurement system for in-process mechanical parts. Advances in Mechanical Engineering, 2017, 9 (10), pp. 1-11.

[10] Peng G, Zhang Z, Li W. Computer Vision Algorithm for Measurement and Inspection of O-rings. Measurements, 2016, 94, pp. 828-836.

[11] Prabhu VA, Tiwaria A, Hutabarata W, Throwera J, Turnera C. Dynamic Alignment Control Using Depth Imagery for Automated Wheel Assembly. Procedia CIRP 25 (C), 2014, pp. 161-168.

[12] Min Y, Xiao B, Dang J, Yue B, Cheng T. Real Time Detection System for Rail Surface Defects Based on Machine Vision. EURASIP Journal on Image and Video Processing (3), 2018, pp. 1-11.

[13] Gong L, Lin C, Mo Z, Shen X, Lin K, Liu X, Liu C. A Generic Adaptive Fractal Filtering Algorithm for Identifying Work Piece Defects on Multiple Surfaces. preprints.org 2018. Available on line from: https://www.preprints.org/manuscript/201808.0517/v1. [accessed 3 September 2019].

[14] Wang C, Wang N, Ho M, Chen X, Song G. Design of a New Vision-based Method for the Bolts Looseness Detection in Flange Connections. IEEE Transactions on Industrial Electronics, 2019, early access, pp. 1-1.

[15] Chauhan V, Surgenor B. A Comparative Study of Machine Vision Based Methods for Fault Detection in an Automated Assembly Machine. Procedia Manufacturing (1), 2015, pp. 416-428.

[16] Louw L, Droomer M. Development of a Low Cost Machine Vision Based Quality Control System for a Learning Factory. Procedia Manufacturing (31), 2019, pp. 264-269.

[17] Lies BT, Cai Y, Spahr E, Lin K, Qin, H., 2018. Machine Vision Assisted Micro-Filament Detection for Real-Time Monitoring of Electrohydrodynamic Inkjet Printing. In: Procedia Manufacturing (26), 2018, pp. 29-39.
[18] OpenCV ver. 3.2.0, 2019. Available from: www.opencv.org [accessed 20 August 2019].
[19] PYNQ: Python Productivity for Zynq. Available from: www.pynq.io [accessed 16 September 2019].
[20] Canny JF. A Computational Approach to Edge Detection. In: IEEE Transactions on Pattern Analysis and Machine Intelligence, 1986, 8 (6), pp. 679-698.
[21] Hartley R, Zisserman A. Multiple View Geometry in Computer Vision. 2nd Edition, Cambridge University Press, New York, NY, 2003.